Advanced wavenumber domain processing for reconstruction of broad-beam, multiple-receiver synthetic aperture imagery

H. J. Callow, M. P. Hayes, and P. T. Gough

Acoustics Research Group,
Dept. Electrical and Electronic Engineering, University of Canterbury,
Private Bag 4800, Christchurch
E-mail: {h.callow,m.hayes,p.gough}@elec.canterbury.ac.nz

Abstract

To boost the mapping rate of synthetic aperture sonars (SASs), systems employing multiple hydrophones are used. Images from these multiple-receiver SAS systems are reconstructed from the recorded data using the same algorithms as in single-receiver SAS. Currently the data-sets are converted (via interpolation) into a single-receiver equivalent before reconstruction using the phase centre approximation. Processing multiple-receiver SAS data with single-receiver reconstruction methods causes image blurring and degradation.

In this paper we propose an improved reconstruction method based on the bistatic sonar model. The new method is a refined wavenumber algorithm that avoids the need for the phase centre approximation. The improvement over current methods is significant for systems with many receivers but is traded off against increased processing. More work on the algorithm may show ways of reducing the processing required.

1 Introduction

Synthetic aperture sonar (SAS) is a modification of traditional sonar imaging that promises higher-resolution for a given wavelength, lower power consumption, and lower hardware costs. The disadvantage of SAS is that post-collection processing is required before image formation. Because of the extremely high resolution desired, mapping rate constraints on SAS systems have led to the adoption of multiple-receive-hydrophone systems [1, 2, 3]. A system having N hydrophones (spaced in the direction of travel) allows the sonar to be towed N times faster than a single receiver equivalent. This tow-speed improvement allows the data for very high-resolution SAS images to be acquired at realistic mapping rates.

Currently several fast algorithms are employed for reconstructing SAS imagery, such as the chirp-scaling, wavenumber, and range-Doppler algorithms. Typically these algorithms are designed to operate on single-receiver, single-transmitter data sets and multiple-receiver SAS datasets are pre-processed into single-receiver equivalents [4, 5, 6, 7]. This preprocessing step usually involves an interpolation and a phase correction step. Unfortunately the phase correction required is both range and target aspect variant. As correction is usually applied to focus the centre of the scene, targets at the edge suffer blurring and loss of phase signature [6].

For the SAS systems in use, this blurring is not large compared to the system resolution, thus has little apparent effect. Unfortunately for the next generation of high-resolution SAS systems, offering better than 25x25mm resolution, the current reconstruction techniques will result in image degradation and a significant loss in resolution. The current single-receiver based algorithms will not be able to provide diffraction limited imagery with multiple receiver systems.

As we will show in Section 3, it is possible to include some of the deterministic second order effects in the multiple receiver system model. With this extra information, it is possible to derive improved reconstruction methods able to prevent blurring. We present the derivation of an improved wavenumber domain reconstruction in Section 3 with the preliminary notation and system geometry described in Section 2. We also show how the typical phase-centre assumptions fit into this new framework. In addition, Section 4 covers an as-yet untested method of correcting for in-pulse temporal Doppler effects.

2 System Geometry

The 3D geometry for a standard synthetic aperture sonar system is depicted in Figure 1. A SAS system insonifies a

wide region of sea-floor in the direction perpendicular to the direction of travel. The forward velocity is severely limited by the slow speed of sound propagation in water.

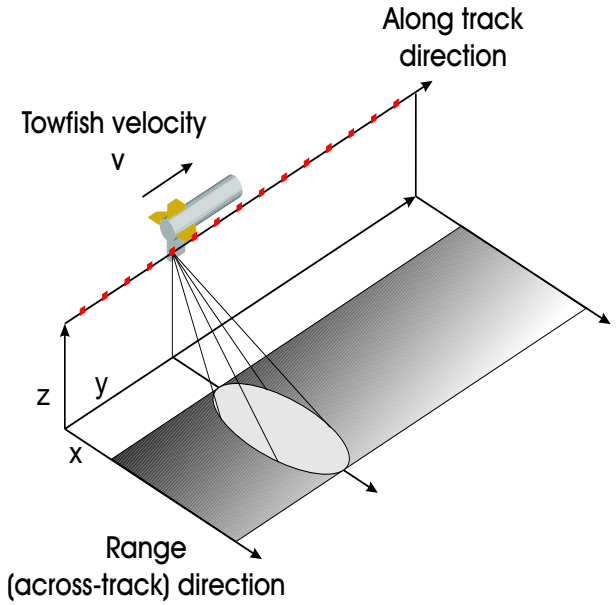

Figure 1. Standard system geometry for a sea-floor mapping SAS system.

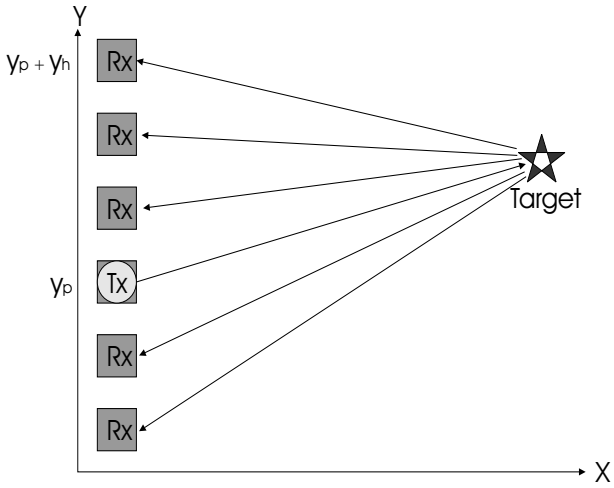

Figure 2. Receiver geometry for a multiple-receiver SAS system.

A multiple receiver sonar is able to travel N times more quickly in the forward direction by taking N samples per sonar ping (one sample per hydrophone). The system geometry for a multiple receiver system is shown in Figure 2.

By using the phase-centre approach we approximate the transmitter / receiver pair of Figure 2 as a single ghost transducer located mid-way between them (an apparent co-located pair). This results in the apparent geometry of Figure 3. The unwanted side-effect of the approximation is an error in the range. Simply put, the round trip range is shorter for the co-located tx / rx pair than the actual round-trip distance. The approximation error, ϵ, due to the assumption of a phase centre sonar is:

$$\begin{aligned}\epsilon =& \sqrt{x^2 + (y_p - y)^2} + \sqrt{x^2 + (y_p + y_h - y)^2} \\ & - 2\sqrt{x^2 + (y_p + y_h/2 - y)^2},\end{aligned} \tag{1}$$

where y_p is the transmitter position, y_h the position of the receiving hydrophone relative to y_p, and x and y are the across-track and along-track position of the target. In a good approximation of (1), the error, ϵ may be written,

$$\epsilon \approx \frac{y_h^2}{4x} - \frac{7}{64}\frac{y_h^4}{x^3}, \tag{2}$$

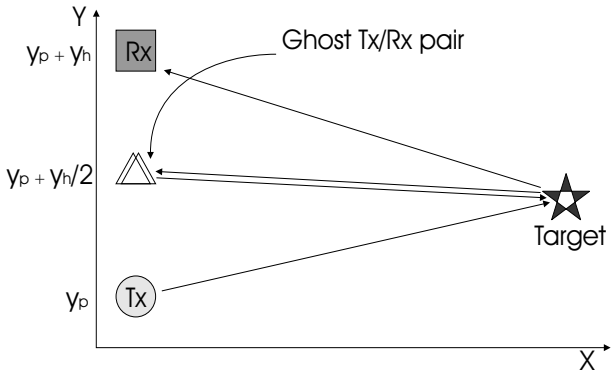

Figure 3. Approximated Receiver geometry of Figure 2 when using the phase centres approach.

by employing the binomial approximation. For a target 25m away from the sonar at broad side, the error of the simulated sonar discussed in Section 5 is up to 9 mm, a significant proportion of the that sonar's 15 mm wavelength.

3 System Model

To model the multiple receiver sonar, we use the space-variant point-spread-function for a *bistatic* sonar,

$$h(x, y, y_h, y_p, f) = H_0^{(2)}(2\pi(f/c)r_p)H_0^{(2)}(2\pi(f/c)r_h), \tag{3}$$

where $H_0^{(2)}$[1] is the zero order Hankel transform of the 2nd kind [8], r_p is given by,

$$r_p = \sqrt{x^2 + (y_p - y)^2}, \tag{4}$$

r_h is given by

$$r_h = \sqrt{x^2 + (y_p + y_h - y)^2}, \tag{5}$$

f/c is the wave speed, and y_p, y_h the positions of the projector and hydrophone respectively. Taking the spatial Fourier of (3) Transform using Weyl's identity [8, 9], gives the wavenumber-domain spatial-impulse response,

$$H\big(x, y, f_{y_h}, f_{y_p}, f\big) = \frac{\exp\left(-j2\pi\,|x|\left(\sqrt{(f/c)^2 - f_{y_h}^2}\sqrt{(f/c)^2 - (f_{y_p} - f_{y_h})^2}\right)\right)}{\sqrt{(f/c)^2 - f_{y_h}^2}\sqrt{(f/c)^2 - \big(f_{y_p} - f_{y_h}\big)^2}}. \tag{6}$$

Rewriting the received field using (6), including the range offset x_0, and remembering that due to single side imaging $|x| = x$, gives,

$$\begin{aligned} E\big(f_{y_h}, f_{y_p}, f\big)|_{x=x_0} = & \\ & \frac{\exp\left(-j2\pi x_0\sqrt{(f/c)^2 - f_{y_h}^2}\right)}{\sqrt{(f/c)^2 - f_{y_h}^2}} \\ & \times \frac{\exp\left(-j2\pi x_0\sqrt{(f/c)^2 - \big(f_{y_p} - f_{y_h}\big)^2}\right)}{\sqrt{(f/c)^2 - \big(f_{y_p} - f_{y_h}\big)^2}} \\ & \times \iint ff(x, y)\ \exp\left(-j2\pi f_{y_p} y\right) \\ & \times\ \exp\left(-j2\pi x\sqrt{(f/c)^2 - \big(f_{y_p} - f_{y_h}\big)^2}\right) \\ & \times\ \exp\left(-j2\pi x\sqrt{(f/c)^2 - f_{y_h}^2}\right)\mathrm{d}x\mathrm{d}y. \end{aligned} \tag{7}$$

[1]This is the 2D Green's function.

Recognising the 2D integration of (7) as a 2D Fourier Transform of $ff(x, y)$ gives,

$$E\big(f_{y_h}, f_{y_p}, f\big)|_{x=x_0} = \frac{\mathcal{S}^{-1}\Big\{FF\Big(f_x, f_y\Big)\exp\Big(-j2\pi x_0 f_x\Big)\Big\}}{\sqrt{(f/c)^2 - f_{y_h}^2}\sqrt{(f/c)^2 - \big(f_{y_p} - f_{y_h}\big)^2}}, \tag{8}$$

where x_0 is the across-track distance offset and the mapping $\mathcal{S}^{-1}\{\}$ is the inverse of the Fourier domain change of variables is given by,

$$f_x = \sqrt{(f/c)^2 - f_{y_h}^2} + \sqrt{(f/c)^2 - \big(f_{y_p} - f_{y_h}\big)^2} \tag{9}$$

$$f_y = f_{y_p}. \tag{10}$$

The basis of the improved wavenumber algorithm is to transform the measured data into the wavenumber domain and perform a coordinate transform[2]. At this point, an inverse Fourier Transform can provide an estimate of the seafloor scatterers. This may be summarised as,

$$\begin{aligned} FF\big(f_x, f_y\big) = & \\ & \mathcal{S}\Big\{E\big(f_{y_h}, f_{y_p}, f\big) \\ & \times \sqrt{(f/c)^2 - f_{y_h}^2}\sqrt{(f/c)^2 - \big(f_{y_p} - f_{y_h}\big)^2}\Big\} \\ & \times \exp\Big(j2\pi f_x x_0\Big), \end{aligned} \tag{11}$$

where $\mathcal{S}\{\}$ refers to the coordinate transform of (9) and (10) and is performed via a frequency domain interpolation ([10], Stolt mapping [11]). The magnitude correction term, $\sqrt{(f/c)^2 - f_{y_h}^2}\sqrt{(f/c)^2 - \big(f_{y_p} - f_{y_h}\big)^2}$, is often neglected.

3.1 Phase Centres Approximation

When approximating a bistatic sonar using the phase centres approximation, the sonar echos are modelled as being both transmitted and received at a ghost receiver midway between the real transmitter and the real receiver in question. When using the approximation it is possible (see Appendix 1) to show that $f_{y_p} = 2f_{y_h}$. If this is used in (11)

[2]This coordinate transformation is usually implemented via a frequency-domain interpolation.

the reconstruction becomes,

$$FF(f_x, f_y) = \mathcal{S}\Big\{ E(f_{y_h}, f_{y_p}, f) \times \sqrt{(f/c)^2 - (f_{y_h})^2}\sqrt{(f/c)^2 - (f_{y_h})^2} \Big\} \times \exp\Big(j2\pi f_x x_0\Big), \quad (12)$$

where the coordinate mappings of (9) and (10) are now,

$$f_x = 2\sqrt{(f/c)^2 - (f_{y_h})^2} \quad (13)$$

$$f_y = f_{y_p}. \quad (14)$$

Rewriting (10) gives the standard wavenumber reconstruction (for phase centre sonars) [12],

$$f_x = \sqrt{4(f/c)^2 - (f_{y_p})^2}. \quad (15)$$

4 In-Pulse Doppler Correction

Another second order effect, thought to have serious consequences for very high resolution SAS imagery, is that caused by temporal Doppler shifting during the pulse transmission. This occurs in wide-beam sonars travelling at relatively high along-track velocity. Any targets forward of broadside will be Doppler-shifted up in frequency and any behind will be down-shifted. Whilst this will only cause minor blurring[3], geometric distortion occurs resulting in misaligned imagery.

Because the Doppler-shifting is deterministic, it is possible to correct for this misalignment in the wavenumber reconstruction at the interpolation step. Starting with the expression for the received echo frequency for a stationary, broadside target and a moving sonar [13],

$$f_r = f\frac{(c + v_s)}{(c - v_s)}, \quad (16)$$

where v_s is the sonar velocity in the along-track direction, and f_r and f are the received and transmitted frequencies respectively. Generalising for targets off axis (16) becomes,

$$f_r = f\frac{(c + v_s \sin(\theta))}{(c - v_s \sin(\theta))}, \quad (17)$$

where θ is the angle of the target from the beam axis. Noting that $f_y = f \sin\theta$ we can get an expression for the received frequency in terms of the sonar velocity and along-track spatial frequency[4]:

$$f_r = f\frac{(c + v_s f_y/f)}{(c - v_s f_y/f)}. \quad (18)$$

Equation (18) may then be used (by substituting f_r for f in the Stolt mapping of (9) and (10) to allow the reconstruction to correct any unwanted Doppler effects. The supposed external information of the sonar velocity, v_s, is normally required for reconstruction purposes anyway. With the substitution of f_r for f (9) and (10) will be:

$$f_x = \sqrt{\left(\frac{f + v_s f_{y_p}/c}{f - v_s f_{y_p}/c}\right)^2 - f_{y_h}^2} + \sqrt{\left(\frac{f + v_s f_{y_p}/c}{f - v_s f_{y_p}/c}\right)^2 - (f_{y_p} - f_{y_h}^2)}, \quad (19)$$

$$f_y = f_{y_p}. \quad (20)$$

Equations (19) and (20) should also be able to be implemented as a Fourier domain change of variables.

5 Results

For simulation purposes we are dealing with a hypothetical system approximately matching the specifications of the 2nd generation US Navy sonar [14]. This system has 32 receivers evenly spaced over a 2 metre array. The platform is to be towed at 7 knots (3.5 m/s). Each of the transducers has the same along track extent of 0.0625 m, this sets the theoretical along-track resolution at 0.0312 m. The transmitted signal has a 20 kHz bandwidth at a centre frequency of 100 kHz, setting the range resolution at 0.0254 m. The sonar system is capable of this resolution from 5 m range out to about 500 m.

To test the new proposed algorithm, the echos scattered by a single-point target using the system described above were simulated. The target is centred at 25 m from the sonar track so it is at the extreme near range of the operating envelope.

Figure 4 shows some of the raw received echo data from the middle hydrophone. This image is extremely undersampled and unable to provide useful reconstructed imagery by itself. When the images from all 32 hydrophones are combined using the phase centre approach, the reconstruction provides the image of Figure 5. Note the splitting of the main lobe into many apparent targets. Distortion of this type has an extremely severe effect on typical imagery.

If we instead reconstruct with the proposed algorithm, the image of Figure 6 is the result. A much cleaner main

[3]The blurring is caused by temporal decorrelation in the pulse compression stage.

[4]For simplicity we use f_y as the along-track spatial frequency. Following the analysis of Section 3, transmit and receive spatial frequencies should be treated separately.

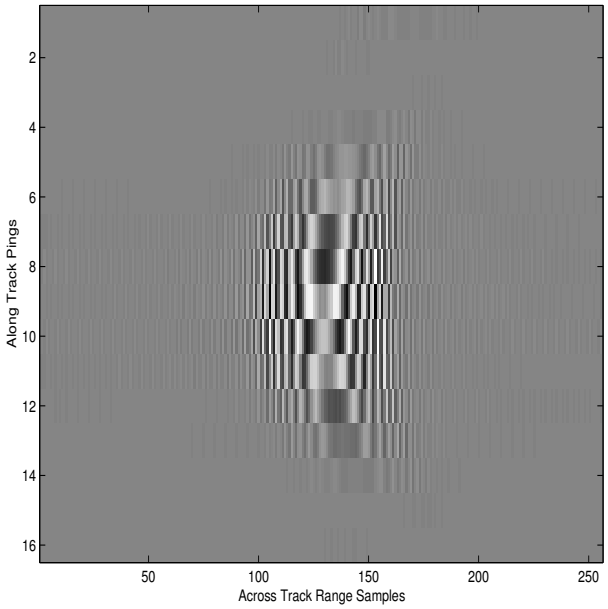

Figure 4. Real part of raw echo data from a single hydrophone in an array of 32.

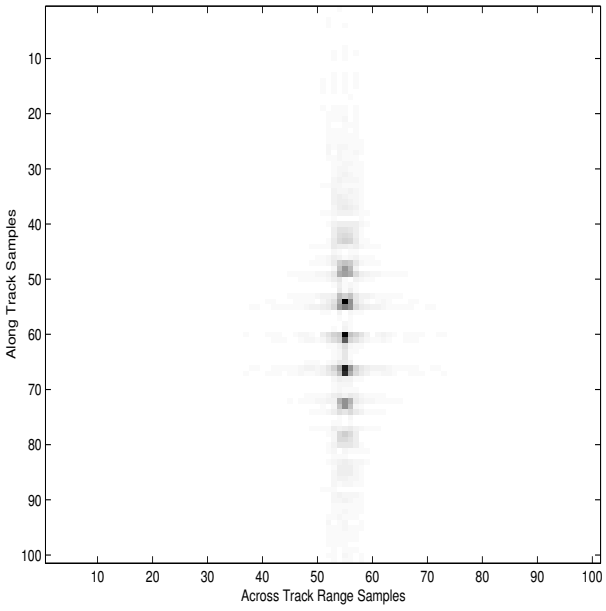

Figure 5. Reconstructed image of single point reflector using the phase centres approach of (12).

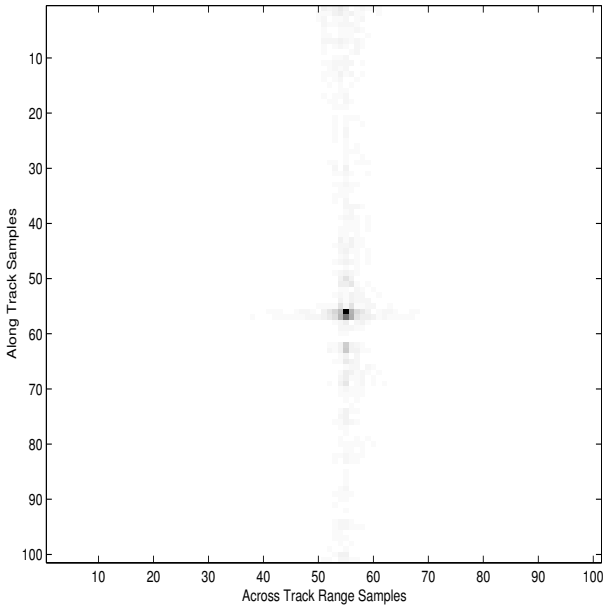

Figure 6. Reconstructed image of single point reflector using proposed algorithm (11).

lobe exists. Although not apparent in the images presented, the new algorithm has a significantly altered side-lobe structure. The cause for this is not readily apparent. Whilst the result is better than the unmodified phase centres method, the side-lobes currently are approximately 6 dB higher than expected.

6 Conclusions

Current multiple-receiver reconstruction methods based on single-receiver algorithms cause unwanted blurring of images. By more accurately modelling the imaging process we have been able to propose an improved reconstruction technique. To get the improved reconstruction, additional processing is required, although the method is still computationally much less demanding than time-domain correlation techniques. The technique has promise for utilisation in the SAS field were the fast algorithms have not had the anticipated acceptance, partly due to poor reconstruction results. At present images reconstructed using the new method have higher side-lobes than expected (most likely due to spatial aliasing effects). We are currently investigating techniques for reducing this problem.

Appendix A

This section details the spatial frequency coverage of a phase centre sonar system. Starting with the phase centre data: the ranges, r_h and r_p, (cf. (4), (5)) used in (3) become,

$$r_h = r_p = \sqrt{x^2 + (y_p + y_h/2 - y)^2}. \tag{21}$$

Using Weyl's identity to perform the Fourier integral over y_p in (3) with (21) substituted for r_p, r_h gives,

$$\begin{aligned} H\big(x, y_h, f_{y_p}, f\big) = \\ \frac{\exp\left(-j2\pi\,|x|\,\left(\sqrt{4(f/c)^2 - f_{y_p}^2}\right)\right)}{\sqrt{4(f/c)^2 - f_{y_p}^2}} \\ \times \exp\big(-j2\pi f_{y_p}(y - y_h/2)\big). \end{aligned} \tag{22}$$

Using the Fourier shift theorem on (22) gives,

$$\begin{aligned} H\big(x, f_{y_h}, f_{y_p}, f\big) = \\ \frac{\exp\left(-j2\pi\,|x|\,\left(\sqrt{4(f/c)^2 - f_{y_p}^2}\right)\right)}{\sqrt{4(f/c)^2 - f_{y_p}^2}} \\ \times \exp\big(-j2\pi f_{y_p} y\big) \\ \times \delta\big(f_{y_h} - f_{y_p}/2\big). \end{aligned} \tag{23}$$

The $\delta\big(f_{y_h} - f_{y_p}/2\big)$ term in (23) means data from phase centre sonars only exists on the line in Fourier space where $2f_{y_h} = f_{y_p}$.

References

[1] R. W. Sheriff, "Synthetic aperture beamforming with automatic phase compensation for high frequency sonars," in *Proceedings of the 1992 Symposium on Autonomous Underwater Vehicle Technology*, pp. 236–245, IEEE, 1992.

[2] B. L. Douglas and H. Lee, "Synthetic-aperture sonar imaging with a multiple-element receiver array.," in *IEEE Internation conference on Acoustics, Speech, and Signal Processing*, vol. 5, pp. 445–448, IEEE, April 1993.

[3] V. Tonard and M. Brussieux, "Towards development of autofocusing schemes for phase compensation of synthetic aperture sonars," in *OCEANS 1997*, vol. 2, (Nova Scotia, Canada), pp. 803–808, IEEE, October 1997.

[4] M. P. Hayes and P. T. Gough, "Imaging with a multiple-hydrophone synthetic aperture sonar," in *Image Vision Computing New Zealand 1999*, IVCNZ, 1999.

[5] J. B. Pat, "Synthetic aperture sonar image reconstruction using a multiple-receiver towfish," Master's thesis, Department of Electrical and Electronic Engineering, University of Canterbury, March 2000.

[6] D. R. Wilkinson, "Effiecient image reconstruction techniuqes for a multiple-receiver synthetic aperture sonar," Master's thesis, Department of Electrical and Electronic Engineering, University of Canterbury, April 2001.

[7] P. T. Gough, M. P. Hayes, and D. R. Wilkinson, "An efficient image reconstruction algorithm for a multiple hydrophone array synthetic aperture sonar," in *ECUA 2000*, pp. 395–400, ECUA, July 2000.

[8] P. M. Morse and H. Feshbach, *Methods of Theoretical physics*, vol. 1. McGraw Hill, 1953.

[9] W. C. Chew, *Waves and Fields in Inhomogeneous Media*. IEEE Press, 1995.

[10] M. Soumekh, *Fourier Array Imaging*. Englewood Cliffs, NJ: Prentice Hall, 1994.

[11] D. W. Hawkins, *Synthetic Aperture Imaging Algorithms: with application to wide bandwidth sonar*. PhD thesis, Department of Electrical and Electronic Engineering, University of Canterbury, October 1996.

[12] P. T. Gough and D. W. Hawkins, "Imaging algorithms for a strip-map synthetic aperture sonar: Minimizing the effects of aperture errors and aperture undersampling," *IEEE Journal of Oceanic Engineering*, vol. 22, pp. 27–39, January 1997.

[13] M. P. Hayes, *A CTFM Synthetic Aperture Sonar*. PhD thesis, Department of Electrical and Electronic Engineering, University of Canterbury, September 1989.

[14] H. Keeter, "Navy awards northrop grumman $3.5 million synthetic aperture sonar contract," *Defense Daily*, vol. 209, March 2001.